Journal of Sound and Vibration (2000) **232**(4), 695–702
doi:10.1006/jsvi.1999.2772, available online at http://www.idealibrary.com on IDEAL®

STARTING JET–WALL INTERACTION

A. SZUMOWSKI, G. SOBIERAJ, W. SELEROWICZ AND J. PIECHNA

Warsaw University of Technology, Institute of Aeronautics and Applied Mechanics, ul. Nowowiejska 24, 00-665 *Warsaw, Poland*

(*Received* 3 *June* 1999, *and in final form* 10 *October* 1999)

A flow starting from a shock tube is accompanied by a bow shock wave and a head ring vortex. This flow pattern is responsible for impulsive sound generation when the jet impinges on the wall. This problem is studied experimentally and theoretically in the present paper. In the experiment a conventional shock tube of internal diameter $D = 65$ mm is used. The jet issuing from the shock tube was visualized by means of a Schlieren system. The instantaneous pressure was measured at the wall at several distances from the axis of the jet. Subsonic and slightly underexpanded jets with flow Mach numbers in the range from 0·65 to 1·14, were considered. It was found that the shock wave, after reflection at the wall, generates a toroidal sound wave due to its interaction with a ring vortex. The sound wave splits into two pressure pulses when it passes through the vortex core. The vortex alone generates a sound wave when it reaches the wall. The theoretical approach is based on the Euler equation. It allowed the authors to predict the main characteristics of the considered flow satisfactorily.

1. INTRODUCTION

High-velocity compressible flows are often accompanied by shock waves and strong vortices. Both structures induce secondary flow effects, e.g., sound waves, when one passes through the other. This phenomenon appears in numerous external and internal flows, e.g., for cascade blades operating at high-subsonic or supersonic Mach numbers; a shock that occurs at a low-pressure blade surface may interact with the vortex street from the preceding blade. Another example is an underexpanded jet flow where a shear layer vortex row periodically passes through the shock wave pattern of the jet.

In the past the theoretical and experimental investigations [1–5] of the shock wave–vortex interaction were performed mostly for a plane shock wave and a cylindrical vortex. A starting vortex shed from the trailing edge of the airfoil when the shock wave passes over it was used in the experiments. Theoretical studies were based on the Euler equation. It allows the investigators to predict both the sound wave pattern and the shock wave deformation during the interaction.

To some extent a different flow pattern appears for the shock wave–vortex interaction in axisymmetric jet flow. In this case the differences, compared to the plane flow, can be expected due to high non-uniform flow velocity distribution in the region of interaction. The ring vortex–shock wave interaction is studied in the present paper for a jet starting from a shock tube. In this case the shock wave is followed by a strong head vortex. After reflection at the opposite wall, the shock interacts with the vortex. An additional effect which appears for the flow considered is the vortex impact on the wall. This effect is also responsible for the sound wave generation.

0022-460X/00/190695 + 08 $35.00/0

2. APPARATUS

A conventional shock tube (see Figure 1) of internal diameter $D = 65$ mm was used in the experiments. A jet starting from the shock tube impinged on a perpendicular wall placed at a distance of two tube diameters. The jet was visualized by means of a Schlieren system in which a spark source of flash or about 1 μs duration was used for illumination. The shock wave Mach number for the shock moving inside the tube was determined by measuring the time required by the shock wave to travel over a test distance of 100 mm. On the basis of the shock wave Mach number the flow Mach number of issuing jet was calculated. The pressure histories were measured at points distributed radially on the impinged wall.

3. NUMERICAL PROCEDURE

The Euler solver in an axisymmetric co-ordinate system was applied to predict the flow properties during the initial phase after the shock wave leaves the shock tube. The control surface shown in Figure 2 was taken into account. Vanishing of the normal velocity at the wall and a Riemann invariant across the expansion wave at the outlet of the shock tube were assumed. For the remaining boundaries of the computational domain the reflectionless conditions were applied. The McCormack predictor–corrector scheme was used [6].

4. RESULTS

The pattern of the considered flow is displayed in Figure 1. The jet from the shock tube is preceded by a bow shock wave which spreads out in the surroundings. The shock wave reflects when it reaches the wall and moves against the jet. The jet appears due to expansion of the air at the outlet region of the shock tube (the air was previously compressed through a shock wave travelling inside the shock tube). The jet is accompanied by a strong head

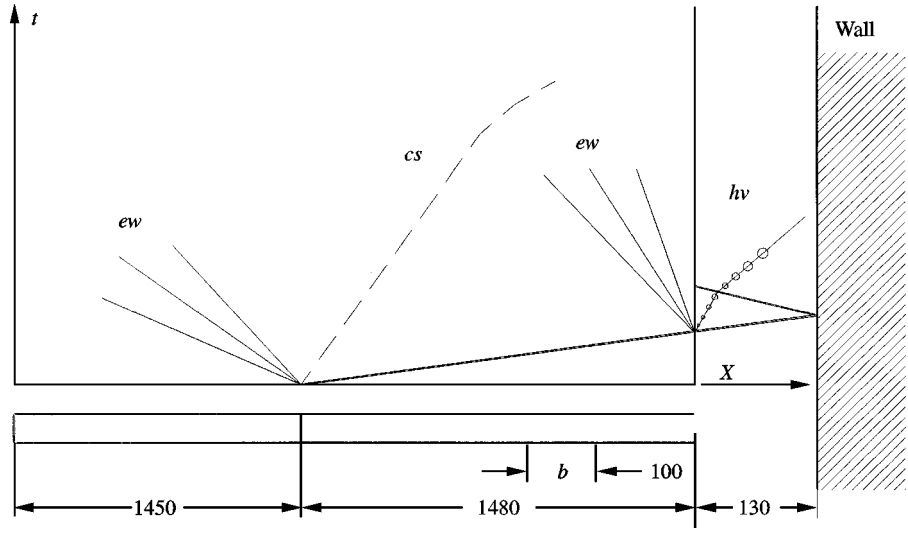

Figure 1. Experimental set-up and phase diagram. sw, Shock wave; ew, expansion wave; hv, head vortex, b, shock speed measured base. Distances in mm.

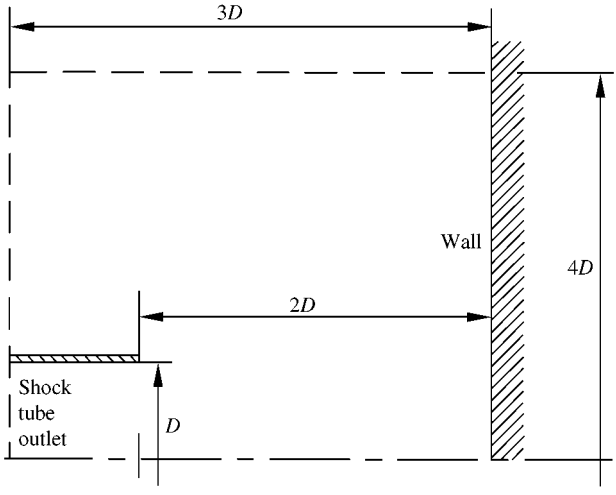

Figure 2. Control surface.

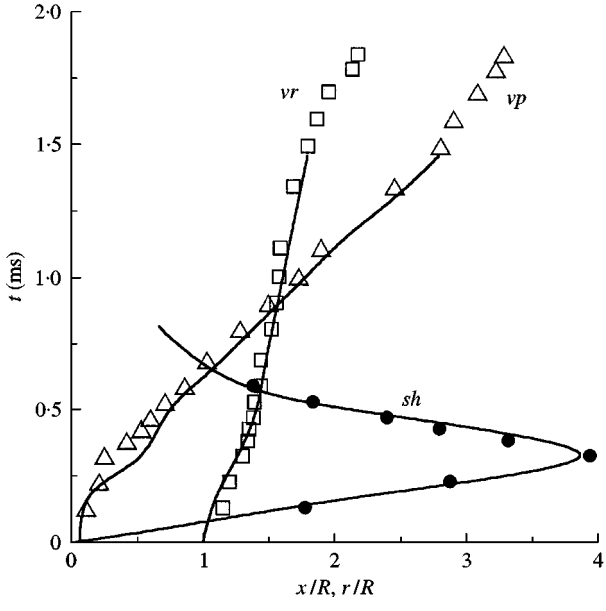

Figure 3. Vortex plane (vp) and shock wave positions (sh) and radius of vortex ring (vr). Jet flow Mach number $M_j = 0{\cdot}65$. Lines, theory; points, experiment.

vortex. The calculated and measured trajectories of the shock wave and the vortex as well as the radius of the vortex ring are shown in Figure 3. The measured values have been taken from flow photographs. A good agreement between predicted and observed trajectories can be noticed.

As was mentioned in the introduction, there are two reasons for impulsive sound wave generation in the flow under consideration: (i) the vortex–shock wave interaction, and (ii) the vortex impact on the wall. These two cases are discussed below in detail.

4.1. VORTEX–SHOCK WAVE INTERACTION

Figure 4 shows the flow photographs corresponding to this case. Photograph (a) shows the reflected shock wave approaching the head vortex. Due to the opposite flow inside the vortex ring the shock is diffracted (photograph (b)) and eventually splits into two parts: one slowly moving against the jet and the remaining one moving outside the jet with undisturbed velocity. The toroidal sound wave distinctly visible in photograph (c) appears to be a product of diffraction.

An additional effect that does not exist in a plane flow, namely the sound wave splitting, is observed in the present flow. This effect, which appears when the sound wave crosses the vortex core, is discussed in detail in Reference [7].

Isobars calculated for four successive phases during the shock wave–vortex interaction process are shown in Figure 5(a)–(d). The concentration of isobars visible in these figures distinctly indicates the shock wave and the vortex positions. Analogous to the experiment, the computed shock wave splitting can be also noticed. The sound wave, being very weak in respect to the shock wave remains, however, undetectable.

4.2. THE VORTEX IMPACT ON THE WALL

The wall pressure varies rapidly when the vortex reaches the wall. Figure 6 shows the pressure histories measured at 10 points distributed radially on the wall. The initial peak of each trace, caused by the shock wave, is followed by pressure variations induced by the jet and the accompanying vortex. For the axis ($r/R = 0$) the pressure, after the shock wave reflection, increases due to increase of the jet flow velocity. The pressure drops subsequently as the vortex rolls off along the wall. Simultaneously at the region where the vortex core approaches the wall, the pressure decreases and then increases. Figure 7 shows the instantaneous pressure distributions for the radial direction extracted from Figure 6. One can notice that the pressure at the radius $r/R = 1{\cdot}5$ remains nearly constant during the initial phase of the vortex–shock wave interaction.

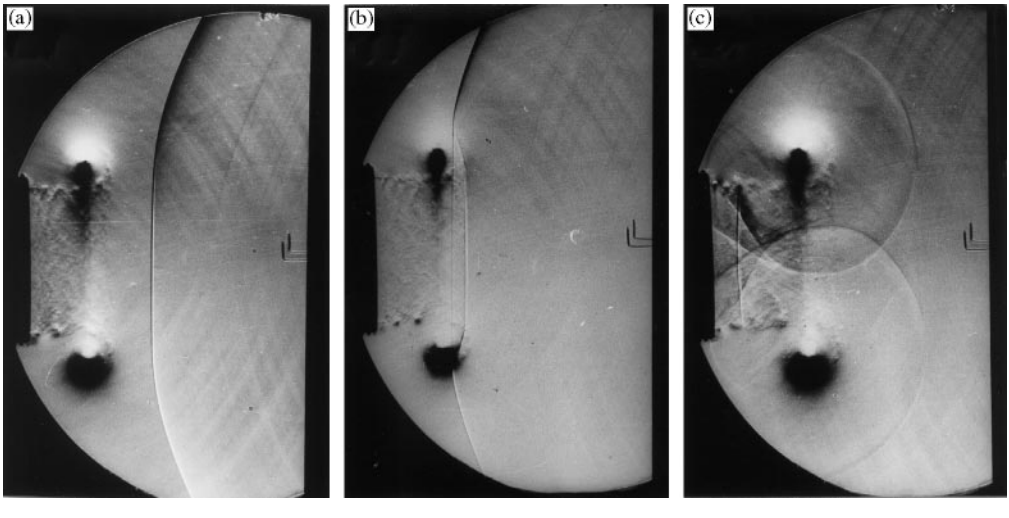

Figure 4. Flow photographs showing successive phases of the ring vortex shock-wave interaction. $M_j = 0{\cdot}65$. Delay time (ms) in relation to the moment when the shock wave leaves the tube: (a) 0·56; (b) 0·615; (c) 0·8.

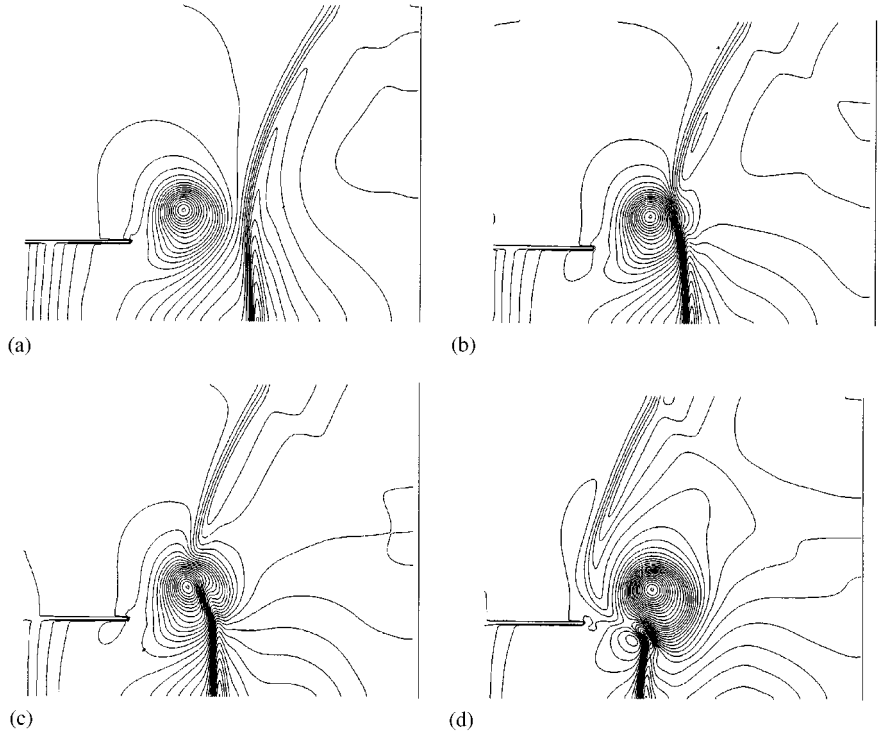

Figure 5. Calculated isobars showing the initial phase of the ring vortex–shock wave interaction. $M_j = 0{\cdot}65$. Delay time (ms): (a) 0·561; (b) 0·613; (c) 0·648; (d) 0·765.

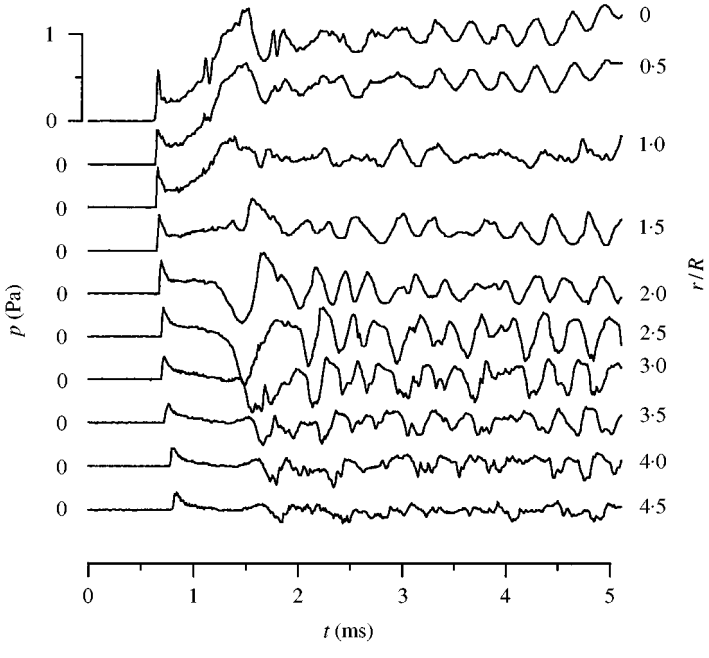

Figure 6. Measured wall pressure histories. $M_j = 1{\cdot}03$. r/R, Pressure transducer positions r normalized with shock tube radius R.

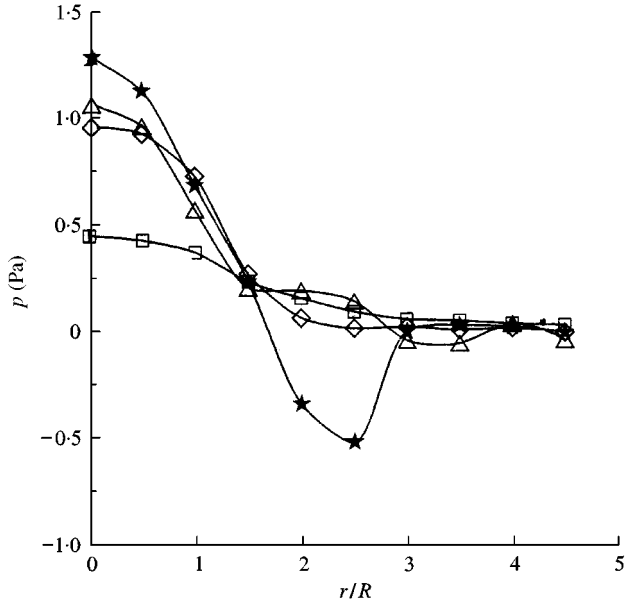

Figure 7. Momentary wall pressure distributions in radial direction. $M_j = 1{\cdot}03$. □, 0·8 ms; ◇, 1·0 ms; △, 1·2 ms; ★, 1·6 ms.

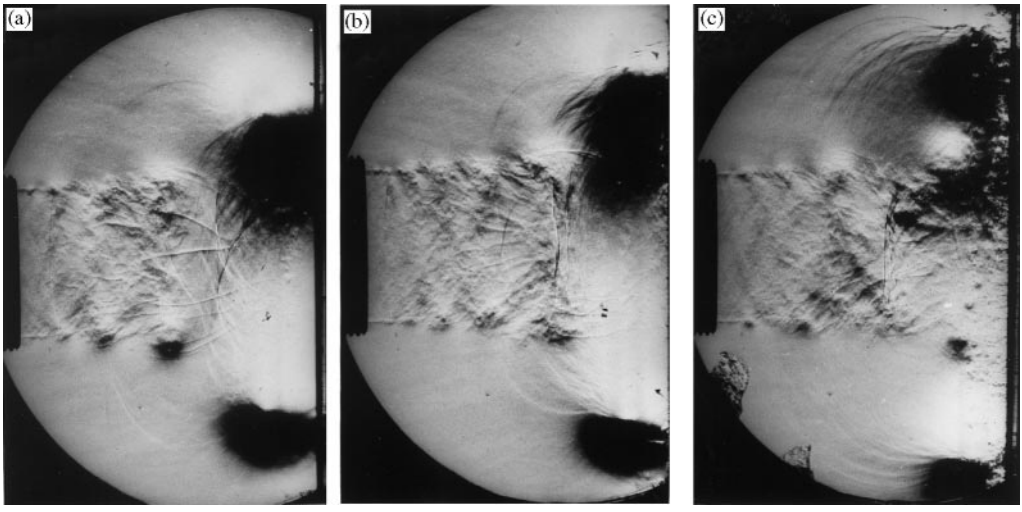

Figure 8. Flow photographs showing successive phases of the ring vortex–wall interaction for subsonic jet. $M_j = 0{\cdot}9$.

The Schlieren photographs of the vortex impact are presented in Figures 8 and 9 for a subsonic and slightly underexpanded jets respectively. The sound wave can be found for both cases considered, in photograph (c) of Figure 8 and in photographs (b)–(d) of Figure 9. It is displayed by toroidal strips in vicinity of the wall. For an underexpanded jet the sound wave is preceded by a weak shock wave front.

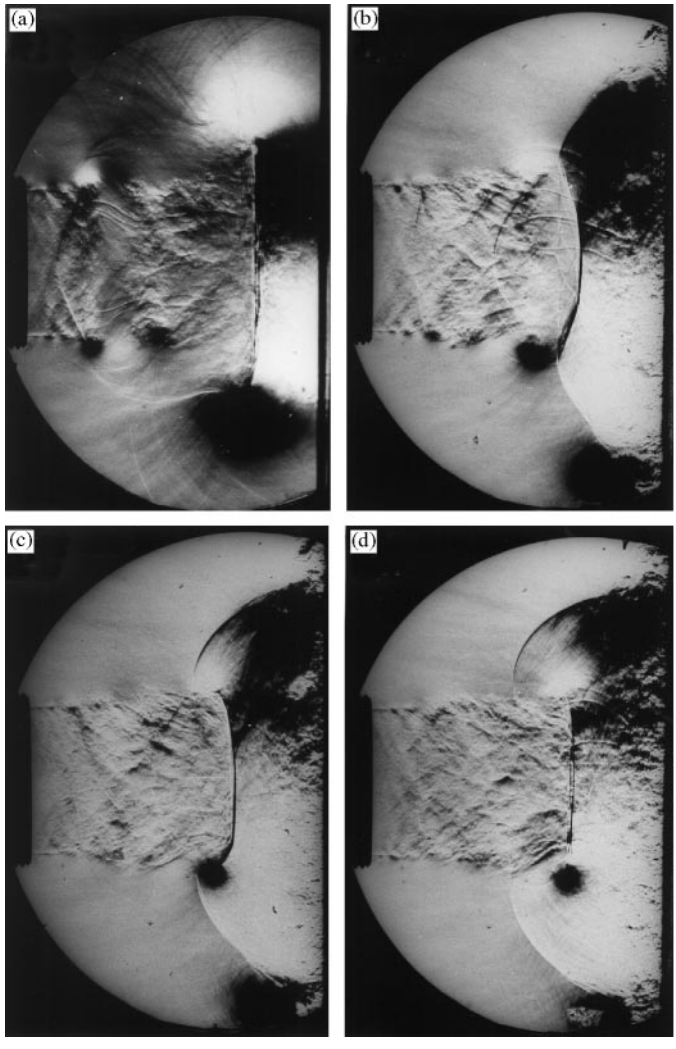

Figure 9. Flow photographs showing successive phases of the ring vortex–wall interaction for underexpanded jet. $M_j = 1{\cdot}14$.

Several secondary ring vortices can be also noted in these figures. They occur due to radial oscillations of the jet which appear as the jet starts.

5. CONCLUSIONS

The starting jet impact on the perpendicular wall provides important observations on the interaction effects of coherent structures, i.e., shock waves and vortices. It was found that a toroidal sound wave is born as the shock passes through the ring vortex. This sound wave splits when it crosses the vortex core.

The vortex itself generates also an impulsive sound wave when it impinges on the wall. For the underexpanded juet the sound wave shows a shock-wave-like front of complicated shape induced by the jet flow.

REFERENCES

1. T. M. WEEKS and D. S. DOSANJH 1967 *American Institute of Aeronautics and Astronautics Journal* **5**, 660–669. Sound generation by shock–vortex interaction.
2. H. S. RIBNER 1973 *American Institute of Aeronautics and Astronautics Journal* **23**, 1708–1715. Cylindrical sound wave generation by shock–vortex interaction.
3. A. NAUMANN and E. HERMANS 1973 *AGARD-CP*-131. On the interaction between a shock wave and a vortex field.
4. D. A. KOPRIVA 1988 *Computational Acoustics*: *Algorithms and Applications* Vol. 2 (D. Lee and M. Schultz, editors). Amsterdam: Elsevier Science Publishers. A multidomain spectral collocation computation of the sound generated by a shock–vortex interaction.
5. K. R. MEADOWS, A. KUMAR and M. Y. HUSSAINI 1991 *American Institute of Aeronautics and Astronautics Journal* **29**, 174–179. Computational study of the interaction between a vortex and a shock wave.
6. C. A. J. FLETCHER 1988 *Computational Techniques for Fluid Dynamics*. New York: Springer-Verlag.
7. A. P. SZUMOWSKI and G. SOBIERAJ 1996 *American Institute of Aeronautics and Astronautics Journal* **34**, 1948–1949. Sound generation by a ring vortex–shock wave interaction.